Published online May 11, 2004

2642–2651 Nucleic Acids Research, 2004, Vol. 32, No. 8
DOI: 10.1093/nar/gkh587

Localization and dynamics of small circular DNA in live mammalian nuclei

Giulia Mearini, Peter E. Nielsen[1] and Frank O. Fackelmayer*

Department of Molecular Cell Biology, Heinrich-Pette-Institute, Martinistraße 52, 20251 Hamburg, Germany and [1]Department of Medical Biochemistry and Genetics, The Panum Institute, University of Copenhagen, Blegdamsvej 3c, DK 2200N, Copenhagen, Denmark

Received February 6, 2004; Revised March 23, 2004; Accepted April 15, 2004

ABSTRACT

While genomic DNA, packaged into chromatin, is known to be locally constrained but highly dynamic in the nuclei of living cells, little is known about the localization and dynamics of small circular DNA molecules that invade cells by virus infection, application of gene therapy vectors or experimental transfection. To address this point, we have created traceable model substrates by direct labeling of plasmid DNA with fluorescent peptide nucleic acids, and have investigated their fate after microinjection into living cells. Here, we report that foreign DNA rapidly undergoes interactions with intranuclear structural sites that strongly reduce its mobility and restrict the DNA to regions excluding nucleoli and nuclear bodies such as PML bodies. The labeled plasmids partially co-localize with SAF-A, a well characterized marker protein for the nuclear 'scaffold' or 'matrix', and are resistant towards extraction by detergent and, in part, elevated salt concentrations. We show that the localization and the low mobility of plasmids is independent of the plasmid sequence, and does not require the presence of either a scaffold attachment region (SAR) DNA element or a functional promoter.

INTRODUCTION

Small circular DNA molecules invade the nucleus of eukaryotic cells during viral infection or the transfection of plasmids, such as vectors for gene therapy. Even though this is a common event, surprisingly little is known about the fate of these molecules in the nuclei of living cells. Import into the nucleus was recently shown to depend on transport through the nuclear pore complex piggybacked on proteins with nuclear localization signals (1). Once inside the nucleus, the incoming foreign DNA acquires a state that facilitates the expression of the enclosed genes. For many viruses, this allows the expression of 'early' genes that stabilize the infection and prepare the host cells for virus replication. Likewise, genes on transfected plasmids are expressed efficiently without requiring a prior integration into the genome. Thus functional interactions of regulatory sequences on the incoming DNA with nuclear components in the host cells can be inferred. However, the mechanism by which this occurs is unclear, as is the question of whether these initial contacts can be modified or abolished (e.g. for therapeutic use).

Interestingly, there is often a difference between the expression of a gene on a transfected vector in transient assays (comparable to an infecting virus genome) compared with the expression of the same gene after the vector has integrated into the genome [reviewed in (2)]. While expression from episomes only depends on the sequence of the regulatory sequences on the vector, the expression of a gene after integration is also affected by its relative position to other genes and its localization in the three-dimensional context of the nucleus.

Certain DNA elements such as scaffold attachment regions (SARs) or boundary elements can alleviate this 'position effect' when present on the integrated vector [reviewed in (3)]. The SAR DNA elements are A+T-rich sequences originally identified by their specific binding to the nuclear scaffold (4,5). In their normal genomic context, SARs are often located close to regulatory sequences such as promoters and enhancers, where they have been shown to affect chromatin accessibility (6) and specific histone modifications associated with transcriptionally active genes (7). A plausible, although not undisputed, hypothesis suggests that SARs exert their effect by tethering chromatin to a proteinaceous nuclear scaffold and organizing the genome into topologically independent loop domains (8). Interestingly, many virus genomes have also been shown to bind to this 'nuclear scaffold', mimicking a host chromatin domain, and depend on this interaction for productive infection [see (9), and references cited therein]. To this end, some viruses carry their own SAR on the genome (10–14), whereas others encode a protein that acts as a bridge between the genome and the nuclear scaffold (15,16) or preferentially integrate into the host genome close to SAR DNA sequences (17,18). These findings have recently been exploited in the rational design of a non-viral vector, where a SAR is sufficient to enable episomal replication and exert mitotic stability, and effectively block the integration of the vector into the genome (19–21). Thus SARs and their interaction with the nuclear scaffold appear to be necessary to maintain a chromatin conformation that facilitates position-independent gene expression [reviewed in (3)]. From hybridization studies on fixed cells, the genomes of SV40

*To whom correspondence should be addressed. Tel/Fax: +49 48051 300; Email: Frank@Fackelmayer.de

 © Oxford University Press 2004; all rights reserved

and adenovirus, as well as plasmid DNA, seem to be heterogeneously distributed in the nucleus, sometimes enriched in the vicinity of nuclear speckles, and excluded from nucleoli (22,23). These results could be compatible with an attachment of the DNA molecules to a nuclear scaffold, and prompted us to devise a method to investigate their localization and dynamics in living cells. Here, we report experiments with fluorescence-labeled plasmid DNA as a model substrate for viral genomes or gene therapy vectors. Peptide nucleic acids (PNAs) were chosen to attach a fluorescent label to the plasmids under investigation. PNAs are synthetic DNA analogs with a pseudopeptide (polyamide) backbone instead of the natural sugar phosphate backbone (24) [reviewed in (25)]. They hybridize to complementary DNA with very high specificity and stability (26) and are not susceptible to degradation by cellular nucleases and peptidases (27). Furthermore, homopyrimidine PNA oligomers form extremely stable helix invasion complexes with complementary targets in duplex DNA (24,28,29), allowing non-covalent but yet very stable labeling of DNA molecules for *in vivo* tracking (30). Owing to the specificity and stability of their interaction with DNA, peptide nucleic acids have attracted much interest as a basis of gene-targeted drugs [reviewed in (31)]. Here, we have utilized these features to allow, for the first time, investigation of the localization and mobility of small circular DNA molecules in the nucleus of the living cell.

MATERIALS AND METHODS

Cell culture and microinjection

COS7 cells (ATCC CRL-1651) were cultivated on plastic dishes in Dulbecco's modified Eagle's medium (DMEM) with 10% fetal calf serum in a humidified atmosphere containing 5% CO_2, and were split 1:5 every second day. For microinjection, cells were seeded onto coverslips containing a 175 µm grid (CeLLocate, Eppendorf, Hamburg) 1 day before injection. Microinjection into the cell nucleus was performed in CO_2-independent medium (Gibco, 18045) with an Eppendorf 5242 microinjector at an average injection pressure of 100 hPa for 0.5 s. Under these conditions, ~0.3 pl was injected per cell; at least 50 cells were injected per experiment. For co-microinjection with expression vectors, labeled DNA and expression vector DNA were mixed in a ratio of 1000:1.

Live cell microscopy

For live cell microscopy, cells were split onto glass-bottomed culture dishes (Mattek), microinjected 1 day after splitting and analyzed 18–20 h later. Cells were placed onto a heated stage at 37°C for analysis with a Zeiss Meta-510 confocal laser scanning microscope. Fluorescence recovery after photobleaching (FRAP) experiments were performed on the same microscope, using 1500 iterations of bleaching with light of 543 nm wavelength for rhodamin-labeled DNA, or 20 iterations at 488 nm for enhanced green fluorescent protein (EGFP) fusion proteins.

Plasmids

Plasmids used in our studies include pMII, containing the human SAR-DNA MII in pBluescript SK+ (32), pK2, a non-expressing complete cDNA clone of SAF-A in pBluescript SK+ (33), the bacterial expression vector pRSET-A (Invitrogen), and the episomally replicating vector pEPI-1, containing a functional promoter and a SAR-DNA element (20). All plasmids contain a unique *Eco*RI restriction site that was used for insertion of the PNA target sequence.

Cloning and labeling of plasmid DNA by PNA

The PNA binding sequence was introduced into the unique EcoRI restriction site of investigated plasmids by cloning of two annealed complementary oligonucleotides (oligo1, AATTGGATCCGAGAAGAAAA; oligo2, AATTTTTT-CTTCTCGGATCC). To allow only a single integration, unphosphorylated oligos were used. All constructs were verified by sequencing and purified by cesium chloride centrifugation. Only preparations with >95% supercoiled plasmid were used for the experiments.

Rhodamine-labeled PNA with the sequence Rh-eg1-KK-JTJTTJTTTT-$(eg1)_3$-TTTTCTTCTC-K-NH_2 (eg1, ethylene glycol linker; K, lysine; J, pseudoisocytosine) was synthesized and purified as described (34), and dissolved in water to a concentration of 100 pmol/µl. For hybridization, PNA was added to 30 µg plasmid at a molar ratio of 50:1 (PNA:DNA) in 120 µl TE, and incubated for 3 h at 37°C. To quantitatively remove unbound PNA, the reaction was then diluted into 2 ml TE and spun in Centricon ultrafiltration units with a 30 kDa cut-off. This washing step was repeated twice before the DNA/PNA complex was concentrated to a final concentration of 0.5–1 µg/µl.

Electrophoretic mobility shift assay

Plasmid DNA (0.75 pmol) was incubated with increasing amounts of rhodamine-labeled PNA in TE (20 µl final volume) at 37°C for 3 h. After incubation, DNA/PNA complexes were digested with restriction enzymes to produce fragments suitable for mobility shift assays. For the experiment in Figure 1, the pMII-plasmid (human SAR element MII in pBluescript, see above) was digested with XbaI and KpnI for 3 h at 37°C. Resulting fragments were analyzed in 1.5% agarose gel to reveal a possible shift of the fragment containing the inserted PNA target sequence.

Sequential extraction of cells

Cells were cultured on glass coverslips coated with 0.1% alcian blue and processed 20 h after microinjection essentially as described previously (35,36). Briefly, cells were incubated with 100 µl CSK buffer (10 mM PIPES pH 6.8, 100 mM NaCl, 300 mM sucrose, 3 mM $MgCl_2$ and 0.5% Triton X-100) for 10 min at room temperature. For better preservation of structure (37), 2 mM sodium tetrathionate was added to the buffer. After washing in phosphate buffer saline (PBS), coverslips were treated for 10 min at room temperature with extraction buffer (10 mM PIPES pH 6.8, 250 mM ammonium sulfate, 300 mM sucrose, 3 mM $MgCl_2$ and 0.5% Triton X-100), washed again in PBS and finally incubated for 10 min at room temperature with 100 µl of 2 M NaCl in the same buffer. Cells were then fixed for 10 min with 3.5% paraformaldehyde and mounted in 40% glycerol in PBS.

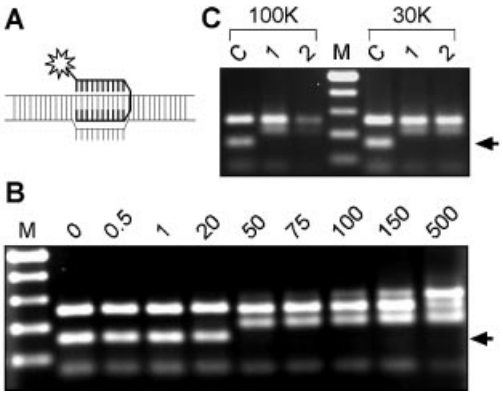

Figure 1. Labeling and purification of plasmid DNA by peptide nucleic acid (PNA). (**A**) Schematic representation of a PNA clamp bound to DNA. One part of the PNA molecule invades the DNA duplex to interact with the complementary DNA sequence according to Watson–Crick hydrogen bonding rules. Via a flexible linker, PNA folds back and the second part of the molecule binds to DNA via Hoogsteen base pairing. The PNA can be labeled with a fluorochrome (star). (**B**) Titration of the optimal PNA:DNA molar ratio for complex formation. Plasmid DNA was incubated with increasing amount of rhodamine-labeled PNA (0–500 molar excess) in TE (20 µl final volume) at 37°C for 3 h. After incubation, DNA/PNA complexes were digested with *Xba*I and *Kpn*I (37°C for 3 h) and resulting fragments were analyzed by 1.5% agarose gel electrophoresis. The arrow indicates the fragment containing the PNA target site; note the complete and exclusive shift of this fragment. M, 100 bp DNA ladder. (**C**) Purification of labeled DNA. After labeling as described in (B), unbound PNA was removed by ultrafiltration over Centricon microconcentrators of 100 or 30 kDa molecular weight cutoff (Millipore). Persistence of the label on the specific fragment was verified by restriction and gel electrophoresis. Note the loss of complexes during the purification with 100 kDa cut-off filters. C, Control DNA with unbound PNA; 1, after labeling but before purification; 2, after purification; M, 100 bp DNA ladder.

Hirt extraction and plasmid quantification

COS7 cells were transfected by electroporation with 10 µg of unlabeled plasmid DNA. Two days after transfection, the medium was removed and the dishes were thoroughly washed with PBS. Cells were then permeabilized by incubation in 3 ml of CSK buffer (see above) for 10 min at room temperature. After two additional washes in PBS, half the dishes were further incubated in 2 M NaCl in 10 mM PIPES pH 6.8, 300 mM sucrose, 3 mM $MgCl_2$ and 0.5% Triton X-100 for 10 min. Cells were then lysed in 3 ml of lysis buffer (0.6% SDS, 10 mM Tris–HCl, 10 mM EDTA) for 5 min, and the lysate was gently mixed with the same volume of 2 M NaCl in TE and stored at 4°C overnight. The next day, precipitated material (containing genomic DNA) was removed by centrifugation at 10 000 *g* for 20 min in the cold. Plasmid DNA was purified from the supernatants by phenol:chloroform extraction and isopropanol precipitation. The DNA pellet was washed in 70% ethanol, air-dried and resuspended in 50 µl of water. Recovered plasmid DNA was quantified by transformation of XL1 Blue bacteria and counting the resulting colonies.

Real-time PCR

Real-time PCR was carried out in a LightCycler (Roche, 2011468) using the LightCycler FastStart DNA Master SYBR Green I kit (Roche, 3003230), with 3 mM $MgCl_2$. Primers suitable for both pBluescript SK+ and pEGFP-C1 were used (forward primer, GTTCCACTGAGCGTCAGACC; reverse primer, CTCAAGTCAGAGGTGGCGAA). The experimental protocol consists of a preincubation at 95°C for 10 min, 40 cycles of amplification (denaturation, 10 s at 95°C; annealing, 10 s at 55°C; elongation, 20 s at 72°C) followed by a melting curve analysis. Hirt supernatants were diluted 1:40 in water and 4 µl was used as template. Each sample was analyzed in duplicate, together with five standards and a negative control. The second derivative maximum method of the LightCycler Software was used for quantification analysis.

RESULTS

Understanding nuclear architecture and its functional role for key genetic processes depends on a detailed knowledge of the localization and dynamic interactions of the involved factors. We have used PNAs to attach a fluorescent label to plasmid DNA, allowing its localization and mobility to be traced in the nuclei of living mammalian cells for the first time. To compare different plasmids, we inserted the 10 bp purine sequence GAGAAGAAAA (1,38) into a variety of vectors and synthesized a universal rhodamine-tagged PNA detector molecule that hybridizes to that region (Fig. 1A). Based on earlier stability measurements, we incorporated pseudoisocytosine into the PNA instead of cytosine to confer pH independence (39), and three lysine residues to increase DNA binding efficiency (40). Conditions of optimal, stoichiometric and specific binding were determined by titration with increasing molar excess of PNA over DNA. After labeling, plasmid DNA was digested with restriction enzymes to generate fragments of suitable size for electrophoretic mobility shift assays and analyzed by agarose gel electrophoresis. We found that a 50-fold molar excess is sufficient for a quantitative and specific binding, as demonstrated by the complete and exclusive shift of the restriction fragment containing the PNA binding site; other fragments were not shifted unless a very high excess of PNA was used (Fig. 1B). After labeling, unbound PNA was removed by two rounds of dilution and ultrafiltration in Centricon microconcentrators, and the labeled DNA was finally concentrated to a concentration of 0.5–1 µg/µl. Interestingly, we consistently lost more than two-thirds of DNA during this purification when microconcentrators with a molecular weight cut-off of 100 kDa were used, but DNA was quantitatively retained using 30 kDa microconcentrators (Fig. 1C). Thus the labeled DNA behaves as expected for a monomeric supercoiled plasmid (41), verifying earlier reports that PNA-labeled DNA does not change its conformation (30). This finding also gives a rough estimate of the effective size of the labeled plasmid in solution, equivalent to a globular protein of between 50 and 100 kDa, and allows a comparison with recently published mobility measurements of dextrans of different sizes (42).

Pilot experiments were performed to devise the best method of introducing the labeled DNA into living cells. As neither electroporation nor chemical transfection were able to yield high enough plasmid numbers to allow visualization *in vivo*, we used microinjection to directly deliver the DNA into the nuclei of cells. We found that ~1500 singly labeled plasmid molecules per nucleus were necessary for microscopic detection, but a more reproducible signal was obtained with a 10-fold increase in copy number. For subsequent experiments, injection conditions were carefully optimized with respect to

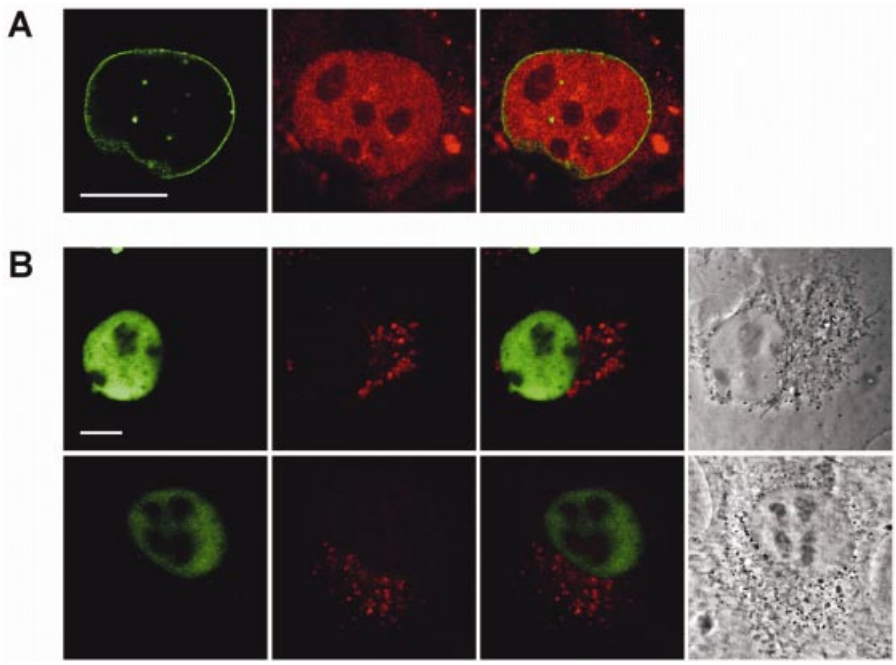

Figure 2. (A) Cell viability after microinjection. COS7 cells grown on coverslips (Eppendorf) were microinjected directly into nuclei with a mixture of DNA/PNA complexes and an expression vector encoding for EGFP-LaminB1. Cells were fixed after 20 h with 3.5% paraformaldehyde and examined by confocal microscopy. Expression and correct localization of the lamin in the nuclear envelope (green) verifies that microinjection does not interfere with vital cellular functions. Note that the injected DNA/PNA complexes (red) remained entirely nuclear. **(B)** Microinjection of free PNA. COS7 cells were injected with a mixture of free rhodamine-labeled PNA and FITC-dextran of molecular weight 250 kDa. Cells were fixed with 3.5% paraformaldeyhde after 1 h (upper panel) or overnight (lower panel) from microinjection. Note that the mixture splits up into its two components, with free PNA (red) completely leaving the nucleus within less than 1 h, while dextran (green) remains nuclear. Scale bar, 10 μm.

cell survival rate by co-injection of an expression vector for EGFP-LaminB1 (Fig. 2A; also compare other expression vectors used in Fig. 5). Under these optimized conditions >80% of injected cells survived and were able to successfully transcribe, translate and transport the reporter gene product. These controls rule out potential toxic side effects of the labeled plasmid and also demonstrate that no vital system of the cell is saturated by the amount of injected plasmid. In addition, injection of a PNA-labeled vector containing a functional EGFP gene resulted in green fluorescent cells, indicating that the expression of a gene encoded by the plasmid is not affected by the tagging (data not shown).

The localization of labeled DNA in injected cells was clearly nuclear, and remained so throughout the experiment (see below), confirming earlier in situ hybridization experiments that had shown the localization of unlabeled plasmids in fixed cells (22). To further verify that nuclear retention was due to the DNA, and not the PNA component, we injected unbound rhodamine-tagged PNA mixed with FITC-tagged dextran of size 250 kDa. Quite unexpectedly, the mixture rapidly split up into its two components, with the PNA leaving the nucleus and forming granular aggregates in the cytoplasm, and the FITC-dextran remaining nuclear (Fig. 2B). The loss of free PNA from the nucleus is fully in line with recent experiments that revealed a strict requirement for a functional NLS to achieve nuclear localization of PNA molecules (43). In the context of our studies, this peculiar behavior of free PNA provided a suitable sensor for the *in vivo* stability of DNA/PNA complexes (see below).

When cells were examined at different time points after injection of PNA-labeled DNA, we found accumulations close to the site of injection for at least 1 h, and it took several hours for the DNA to acquire its final localization (Fig. 3). The fluorescent signal generally remained entirely nuclear throughout the experiment, which included an inspection 3 days after injection. In no case did we observe a significant or even complete reduction of nuclear fluorescence, as in the case of unbound PNA, suggesting that the DNA/PNA complex is very stable *in vivo*. However, additional extranuclear signals were seen in some cells after long incubation times, most probably resulting from a fraction of PNA that has detached from the plasmid and was subsequently exported from the nucleus (Figs 2B and 3).

Subnuclear localization of DNA was examined by confocal microscopy 18–20 h after injection and compared between live and fixed cells. We find that in both cases the localization is quite variable between individual cells, but consistently appears sponge-like due to the presence of some large and numerous smaller areas in the nucleus which do not contain detectable amounts of labeled plasmid (Fig. 4). These regions were identified as nucleoli and PML bodies, respectively, by co-injection of expression vectors encoding GFP-tagged fibrillarin or PML protein (Fig. 5B and C). These proteins localize in the plasmid-devoid regions without significant overlap of fluorescence signals. We noticed, though, that several small nuclear regions contained neither PML protein nor labeled plasmid, and most probably represent nuclear bodies distinct from PML bodies (44). In contrast with the

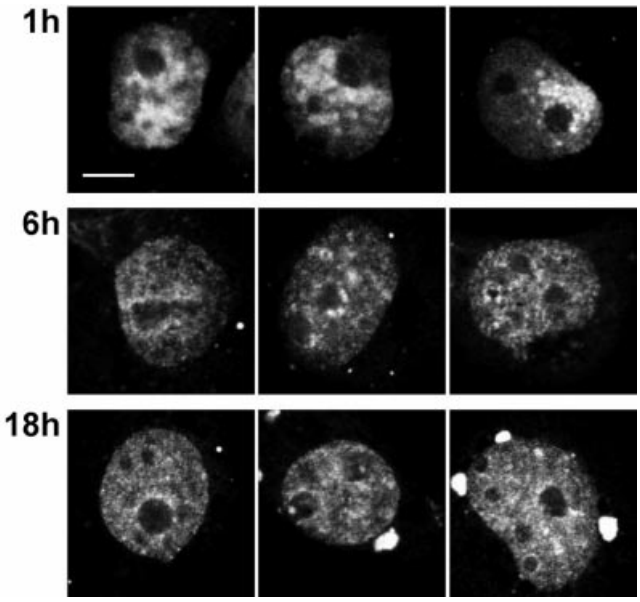

Figure 3. Time course. COS7 cells were microinjected with DNA/PNA complexes into the nucleus, and fixed with 3.5% paraformaldehyde 1, 6 or 18 h after microinjection. Note the heterogeneous distribution 1 h after microinjection. In many cells the point of injection is visible as an accumulation of fluorescence (right panel). After 6 h, the plasmid has reached its final location that does not change further with longer incubation time. Three typical nuclei are shown per time point.

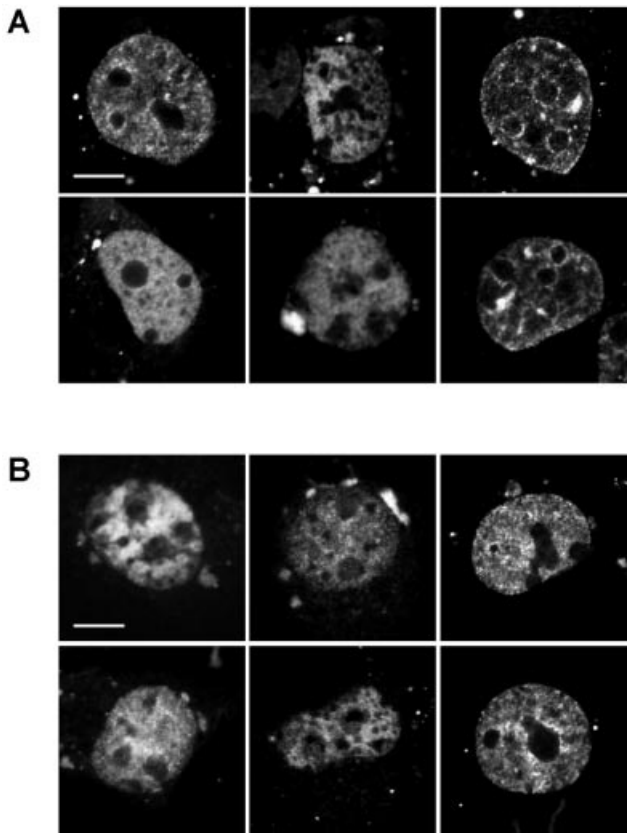

Figure 4. Intranuclear localization of DNA/PNA complexes. COS7 cells were microinjected into the nucleus with DNA/PNA complexes and analyzed by confocal microscopy after **(A)** 18 h alive and **(B)** fixation with 3.5% paraformaldehyde. Six representative nuclei are shown for each. Scale bar, 10 μm.

mutually exclusive localization with nuclear bodies and nucleoli, the localization of the labeled plasmids is very similar to that of SAF-A (Fig. 5A), a well characterized DNA-binding component of the nuclear scaffold known to interact with an episomally replicating plasmid *in vivo* (19,36,45–47).

The co-localization of plasmid DNA with SAF-A, and the long time the plasmids need to acquire their final localization, prompted us to investigate whether the plasmids might become attached to the nuclear scaffold. In a first step, we found that neither the localization nor the intensity of the labeled DNA was significantly affected when the nuclear membrane was removed by treatment with 0.5% Triton X-100, which results in a complete loss of soluble nuclear components (Fig. 6A, left panel). Subsequently, cells were extracted with 2 M sodium chloride, a method routinely used to prepare the 'nuclear matrix' [(48), and references cited therein]. We find, by two different quantification methods, that ~50% of the plasmid was still detectable in the nucleus, but the localization changed to a more granular distribution (Figs 6A, right panel, and 7). This result was independent of the plasmid used, and required neither a SAR nor a functional eukaryotic promoter on the plasmid (Fig. 7). Although surprising, this was consistent with the localization of different plasmids, which also did not reveal any significant difference between SAR- and non-SAR-containing plasmids (Fig. 6B), or a plasmid of entirely prokaryotic sequence (pRSET-A) (data not shown).

As judged by our extraction experiments, plasmid DNA seems quite stably attached to the nuclear scaffold irrespective of its sequence. We confirmed this attachment in living unextracted cells by FRAP experiments. To this end, cells were injected with labeled DNA and expression plasmids

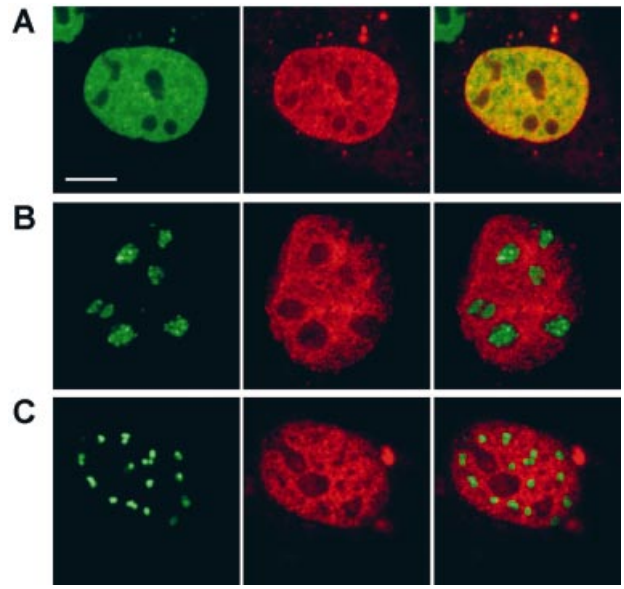

Figure 5. Plasmid DNA does not enter the nucleolus and nuclear bodies. COS7 cells were co-microinjected with DNA/PNA complexes and expression plasmids for **(A)** SAF-A, **(B)** hFibrillarin and **(C)** PML. After overnight incubation, cells were fixed for 10 min with 3.5% paraformaldehyde and examined by confocal microscopy. Note that fibrillarin and PML protein localize at nuclear sites devoid of plasmid DNA, while the localization of plasmid DNA and SAF-A are very similar.

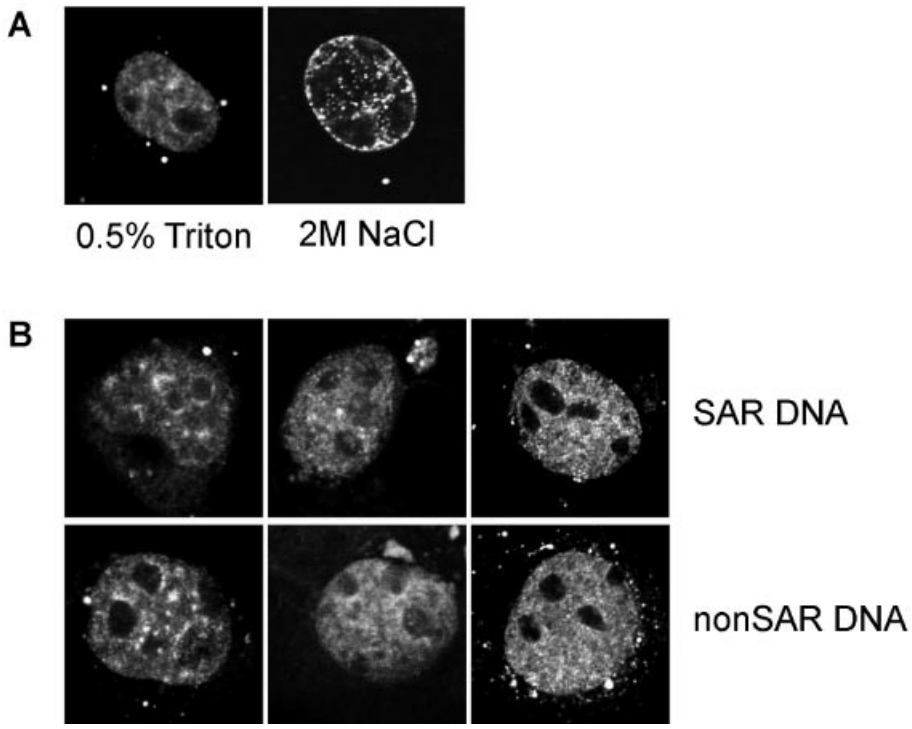

Figure 6. Plasmid DNA is resistant towards detergent extraction and elevated ionic strength, and does not require a SAR DNA element. **(A)** COS7 nuclei microinjected with DNA/PNA complexes were treated with 0.5% Triton X-100 (left) followed by 2 M NaCl extraction (right). The localization after Triton extraction is indistinguishable from that in untreated cells (compare Figs 3 and 5). After high-salt treatment, plasmid DNA is still detectable but has redistributed into intense foci both inside the nucleus and at the nuclear periphery. **(B)** COS7 cells were microinjected with the SAR-containing plasmid pMII or the non-SAR control plasmid pK2. Typical nuclei from both injections are shown, without significant difference between the two constructs.

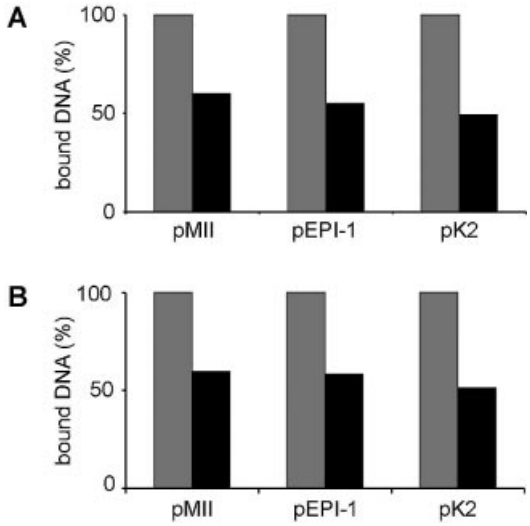

Figure 7. Resistance of transfected plasmid DNA towards high salt. Cells were transfected with three different unlabeled plasmids by electroporation. After 20 h, cells were extracted with Triton X-100 and 2 M NaCl as described in Figure 6 before the remaining plasmids were recovered by the Hirt method. The recovered DNA was quantified by **(A)** transformation of competent bacteria and counting the number of clones and by real-time PCR **(B)**. According to both quantification methods, and independent of the plasmid, approximately half of the plasmid remained bound after 2 M NaCl extraction (black bars) in comparison with untreated cells (grey bars). Results shown here represent the mean of at least three independent experiments, quantified in duplicate each; normalization to the amount of DNA recovered from untreated cells in the same experiment was performed before calculating the mean to compensate for differences in the absolute amount of recovered DNA.

encoding proteins with known mobility; 18 h after injection, narrow strips across the nucleus were photobleached and the recovery of fluorescence from neighboring unbleached regions was monitored over time. We found that fluorescence in the bleached area recovered homogeneously, with no indication of nuclear subcompartments with higher plasmid mobility. Even more interestingly, we did not observe any difference in the mobility of different plasmids. As shown in Figure 8, plasmid DNA is >100-fold slower than a soluble protein of similar dimensions, and fluorescence does not recover completely within 15 min. For quantitative analysis, the loss of fluorescence in a non-bleached reference area of the same nucleus (resulting from a dilution of the fluorescent molecules as they redistribute) was determined, and recovered fluorescence in the bleached area was normalized to the sum of mean intensities in the bleached and unbleached areas. The analysis revealed a mobility curve that is best described as the superposition of a typical first-order recovery curve, such as the one obtained for β-Gal-NLS (Fig. 8D), and a linear increase over time (Fig. 8C). Most probably, this reflects the presence of two populations of plasmid that differ in their mobility: a 'mobile' fraction (comprising ~25–30% of the plasmid), and a larger fraction (70–75%) which is transiently 'immobilized' on a structure and dissociates from there at a constant net rate of ~2%/min. For the mobile fraction, we determined a diffusion coefficient of 4.3×10^{-10} cm^2/s, compared with 2.4×10^{-8} cm^2/s for β-Gal-NLS, an artificial soluble nuclear protein which fully recovers after ~15 s. LaminB1, an immobile component of the nuclear lamina (49)

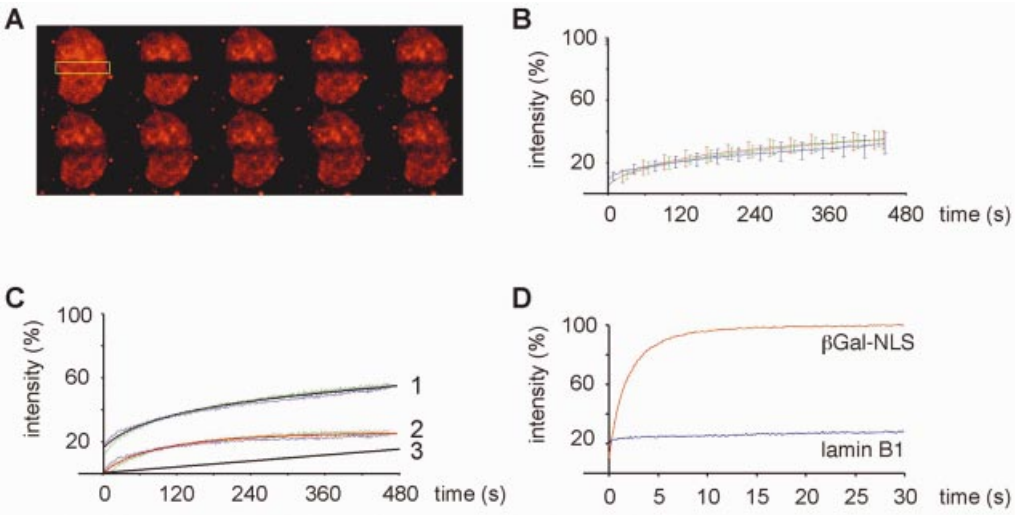

Figure 8. Plasmid DNA is almost immobile in the nucleus. Eighteen hours after microinjection, the intranuclear mobility of plasmid DNA was determined by fluorescence recovery after photobleaching (FRAP) experiments. **(A)** A region of interest (yellow rectangle) was bleached with a high-intensity HeNe laser at 543 nm. Images were taken immediately before photobleaching, and the recovery of fluorescence into the bleached area was monitored over time. Shown here is a typical nucleus with 120 s between the individual images. **(B)** Three different plasmids were investigated and the recovery was quantified from 10 to 20 individual nuclei per construct. Note that the recovery curves are identical, irrespective of the presence or absence of a SAR DNA element or a functional eukaryotic promoter. pMII (green curve), SAR+, promoter–; pEPI-1 (red curve), SAR+, promoter+; pK2 (blue curve), SAR–, promoter–. **(C)** The measured curve (1) can be described as the sum of a typical first-order recovery curve (2) and a linear component (3), suggesting an exchange between the soluble and immobile fractions. Two different plasmids were analyzed here (green, pMII; purple, pK2). **(D)** For comparison, the mobility of βGal-NLS and LaminB1 were determined by FRAP as typical examples of a soluble and an immobile nuclear component, respectively.

does not recover for several hours (Fig. 8D). Thus even the mobile fraction of plasmid DNA has an *in vivo* mobility that is several orders of magnitude lower than anticipated for free diffusion, consistent with a strong, although not completely fixed, attachment to the nuclear scaffold.

DISCUSSION

In this article, we have analyzed the intranuclear localization and mobility of small circular DNA molecules as models for viral genomes and gene therapy vectors. The DNA was specifically labeled by hybridization to a synthetic PNA and microinjected into nuclei of living cells. By this approach, we were able to trace small DNA molecules *in vivo* for the first time, and found that they rapidly associate with nuclear substructures.

Most nuclear components appear to be in constant motion to allow transient interactions between protein factors and *cis*-acting DNA sequences in the genome, and thereby regulate key genetic processes (50). Much insight into the dynamics of these processes was gathered by the use of fluorescent 'tags', such as autofluorescent proteins of the green fluorescent protein (GFP) family [reviewed in (51)]. These proteins can be fused to proteins of interest by simple recombinant DNA techniques, and allow a quantitative determination of protein mobility in live cells in a straightforward way. Much less is known about the dynamics of DNA because it is not yet possible to directly label specific DNA sequences *in vivo*. Indirectly, DNA can be labeled and investigated by the binding of fluorescence-tagged proteins such as GFP-histones to visualize bulk chromatin (52), or by reporter assays where repeats of the bacterial *lac* operator DNA element are detected by a *lac*-repressor:GFP fusion protein (53). These novel labeling methods have shown that genomic DNA, in the form of chromatin, is characterized by both highly dynamic short-range mobility and constrained long-range movements [reviewed in (54)]. Direct metabolic labeling of bulk DNA with fluorescent nucleotide analogs has confirmed these results, and demonstrated that subchromosomal 'foci' move but are detectable as stable entities over several hours (55). These 'foci' appear to be the basic building blocks of interphase chromosomes, which are located in spatially distinct territories without significant overlap to neighboring chromosomes [reviewed in (56)]. The mechanisms that organize chromatin into quite stable 'foci' and, on a higher level, into chromosome territories presumably involve a non-chromatin compartment of the nucleus, often referred to as the nuclear 'matrix' or 'scaffold' (57). Genomic DNA sequences that specifically bind to this entity have been isolated and well characterized, and seem to play important roles in the regulation of gene expression and DNA replication (3,58). However, genes located on experimentally transfected plasmids or infecting virus genomes are also expressed efficiently, even when they do not contain such a 'scaffold/matrix attachment region' (S/MAR) sequence. It therefore appeared desirable to investigate the fate of these small foreign DNA molecules in the nuclei of living cells.

To experimentally address this question, we have specifically labeled plasmid DNA with a fluorochrome-tagged PNA clamp. This appeared to be a promising approach, as a very similar method had earlier provided important insights into nuclear import of plasmids in permeabilized cells (1). The direct labeling technique employed proved suitable for tracking transiently introduced plasmid DNA, a question that could not previously be addressed by established *in vivo* DNA visualization methods such as the indirect *lac*-operator/

repressor system (53). While the *lac*-operator/repressor method is excellent in experiments where the investigated DNA is stably integrated into the genome at one or a few sites, it is not applicable to DNA molecules in transient state. This is mainly due to its dependence on long repeats of binding sites on the DNA, which are inherently unstable and prone to rearrangement, and on the expression of a significant amount of heterologous specific binding protein for indirect detection, which might affect the localization or mobility of DNA in transient assays.

In order to allow an analysis of intact living cells, we delivered the labeled plasmid by microinjection under optimized conditions. The amount of injected plasmid was varied between 0.1 and 1% of the genomic DNA content of the host nucleus, and control experiments revealed that the injection did not compromise the cells, ruling out the possibility that critical systems in the cell might be overloaded or saturated by the injected plasmid. In addition, DNA/PNA complexes appear to be stable in living cells, as we did not observe nuclear export of fluorescence signal characteristic of free unbound PNA (Fig. 2B).

We found that plasmid DNA localizes heterogeneously in the nucleus, with no detectable amount in nucleoli and nuclear bodies such as PML bodies. This result compares well with an earlier study which had investigated the localization of SV40 DNA by in situ hybridization in fixed cells (22) and also found no signals in nucleoli. However, an enrichment in speckle-like subcompartments, as described for SV40 DNA (22), was not particularly evident in our experiments.

The most important result of the studies presented in this article is that circular DNA is not present in soluble freely diffusible form in the nucleus. Rather, immediately after injection, DNA appears to be bound by nuclear substructures that constrain its mobility and render it resistant to treatment with detergents and elevated salt concentrations. This is different from proteins, which can rapidly move in and out of nuclear bodies and exchange with a soluble pool in the nucleoplasm [reviewed in (50)]. FRAP experiments revealed that a subpopulation of plasmid recovers with a diffusion coefficient of 4.3×10^{-10} cm^2/s. This mobility is approximately two orders of magnitude lower than that of typical soluble proteins. However, the vast majority of plasmid is bound to structures that inhibit its movement. Our mobility measurements indicate that bound and mobile plasmids dynamically interchange at a net rate of ~2%/min, accounting for a linear component in the recovery curve. This finding is compatible with our observation that it takes several hours for the plasmid to acquire its final localization, and demonstrates that the plasmids are not invariantly fixed in the nucleus. We cannot formally rule out the possibility that the bound PNA contributes to the localization or low mobility of the labeled plasmid, but consider this unlikely for two reasons. First, PNA-labeled plasmid behaves like a soluble entity of the expected size during ultrafiltration, suggesting that it is not prone to aggregation that could restrict its mobility. Secondly, and more important, quantification of DNA after detergent and high salt treatment (Figs 6A and 7) was performed with unlabeled as well as PNA-labeled plasmids with identical results, demonstrating that PNA does not alter the behavior of the plasmid DNA under study.

The mobility of supercoiled plasmid DNA in live cells has not been investigated before, but can presently only be compared with the mobility of other macromolecules such as proteins or dextrans. Based on the filtration properties described above, our supercoiled plasmids appear to behave equivalently to a globular protein between 30 and 100 kDa. Proteins of this size diffuse almost freely in the nucleus, unless constrained by specific interaction with other nuclear components (59,60). To rule out the effect of such interactions, fluorescence-tagged dextrans of variable size have recently been investigated after injection into the nucleus (42). Not unexpectedly, their mobility decreased from almost free diffusion to immobilization depending on the size of the injected molecule. Mobility compatible with free diffusion was observed for dextrans up to 500 kDa in size, and only significantly larger dextrans were restricted in their mobility. Thus, at comparable size, supercoiled plasmids are much more immobile than dextrans. This finding is also compatible with recent observations of Lukacs and coworkers (61), who investigated the mobility of linear DNA molecules of variable size in the nucleus and cytoplasm.

Presently, we do not know the components that are responsible for the observed immobilization of plasmid DNA inside the nucleus. However, the resistance towards detergents and high salt solutions, as well as the partial co-localization with SAF-A, suggest an involvement of the nuclear 'matrix' or 'scaffold'. This interpretation is compatible with earlier reports on the presence of between 20 000 and 60 000 binding sites for DNA per nucleus in matrix preparations (62–64), which is significantly higher than the number of plasmid copies injected in our experiments. The proteins that supply these binding sites have not been identified, but it is very likely that a variety of different factors such as matrix-associated transcription factors are involved (65). This is supported by careful titration studies that revealed different sets of binding sites for superhelical plasmids and single-stranded DNA on isolated nuclear scaffolds (64). Interestingly, one set of binding sites identified in this study specifically interacts with plasmid with superhelical density <0.04, and has topoisomerization activity. This suggests that topoisomerase II, a well known component of isolated nuclear scaffold, might be involved in binding to superhelical DNA also *in vivo*. However, more recent work has indicated that topoisomerase II behaves as a soluble protein *in vivo* (66), arguing against its involvement in the immobilization of plasmids described in this paper. We found that plasmids that carry a functional eukaryotic promoter (such as pEPI) and plasmids that are entirely prokaryotic in sequence (such as pRSET) revealed no difference in either localization or mobility. Therefore attachment to nuclear substructures does not appear to result directly from gene expression, where active, matrix-bound RNA polymerase II could tether the plasmid to the matrix or transcription 'factories' (67–69). Importantly, we also failed to detect a requirement for SAR DNA elements, which are thought to represent the genomic attachment sites to the nuclear matrix. It is therefore unlikely that SAR binding proteins such as SAF-A (36,45,47) or SAF-B (35,70) are predominantly responsible for immobilizing plasmid DNA. This is particularly noteworthy because one of the vectors used in the present paper, pEPI-1, was recently demonstrated to be bound to SAF-A

in vivo after many generations of episomal replication (19–21). In this case, the SAR DNA element on the vector, and its interaction with SAF-A, was essential for episomal replication and for blocking its integration into the genome.

Future experiments will address the nature of the proteins that affect the localization and mobility of plasmid DNA. Tagged PNA clamps will be a valuable tool for interaction screening of nuclear proteins, and will allow specific enrichment for the involved factors that can then be identified by mass spectrometry. Understanding the molecular mechanism that tethers plasmids to the nuclear matrix, and thereby creates a permissive environment for the expression of the enclosed genes, might allow the rational design of compounds to block this interaction. Possibly, this will later enable inhibition of the expression of some viral genes and attenuate viral infections.

ACKNOWLEDGEMENTS

The authors thank Jan Ellenberg (EMBL, Heidelberg, Germany), Thomas Hofmann (Heinrich-Pette-Institute, Hamburg, Germany) and Ulrich Scheer (University of Würzburg, Germany) for their generous gifts of expression vectors, and Hans-Joachim Lipps (University of Witten-Herdecke, Germany) for the pEPI-1 vector. G.M. was supported by a personal fellowship of the Istituto Pasteur, Fondazione Cenci Bolognetti, University of Rome 'La Sapienza'.

REFERENCES

1. Wilson,G.L., Dean,B.S., Wang,G. and Dean,D.A. (1999) Nuclear import of plasmid DNA in digitonin-permeabilized cells requires both cytoplasmic factors and specific DNA sequences. *J. Biol. Chem.*, **274**, 22025–22032.
2. Bode,J., Goetze,S., Ernst,E., Huesemann,Y., Baer,A., Seibler,J. and Mielke,C. (2003) In Bernardi,G. (ed.), *Gene Transfer and Expression in Mammalian Cells*. Elsevier, Amsterdam, Vol. 38, pp. 551–572.
3. Bode,J., Benham,C., Knopp,A. and Mielke,C. (2000) Transcriptional augmentation: modulation of gene expression by scaffold/matrix-attached regions (S/MAR elements). *Crit. Rev. Eukaryot. Gene Expr.*, **10**, 73–90.
4. Mirkovitch,J., Mirault,M.E. and Laemmli,U.K. (1984) Organization of the higher-order chromatin loop: specific DNA attachment sites on nuclear scaffold. *Cell*, **39**, 223–232.
5. Cockerill,P.N. and Garrard,W.T. (1986) Chromosomal loop anchorage of the kappa immunoglobulin gene occurs next to the enhancer in a region containing topoisomerase II sites. *Cell*, **44**, 273–282.
6. Jenuwein,T., Forrester,W.C., Fernandez-Herrero,L.A., Laible,G., Dull,M. and Grosschedl,R. (1997) Extension of chromatin accessibility by nuclear matrix attachment regions. *Nature*, **385**, 269–272.
7. Martens,J.H., Verlaan,M., Kalkhoven,E., Dorsman,J.C. and Zantema,A. (2002) Scaffold/matrix attachment region elements interact with a p300-scaffold attachment factor A complex and are bound by acetylated nucleosomes. *Mol. Cell. Biol.*, **22**, 2598–2606.
8. Gasser,S.M. and Laemmli,U.K. (1987) A glimpse at chromosomal order. *Trend Genet.*, **3**, 16–22.
9. Deppert,W. and Schirmbeck,R. (1995) The nuclear matrix and virus function. *Int. Rev. Cytol.*, **162A**, 485–537.
10. Jankelevich,S., Kolman,J.L., Bodnar,J.W. and Miller,G. (1992) A nuclear matrix attachment region organizes the Epstein-Barr viral plasmid in Raji cells into a single DNA domain. *EMBO J.*, **11**, 1165–1176.
11. Pommier,Y., Cockerill,P.N., Kohn,K.W. and Garrard,W.T. (1990) Identification within the simian virus 40 genome of a chromosomal loop attachment site that contains topoisomerase II cleavage sites. *J. Virol.*, **64**, 419–423.
12. Mearini,G., Chichiarelli,S., Zampieri,M., Masciarelli,S., D'Erme,M., Ferraro,A. and Mattia,E. (2003) Interaction of EBV latent origin of replication with the nuclear matrix: identification of S/MAR sequences and protein components. *FEBS Lett.*, **547**, 119–124.
13. Stunkel,W., Huang,Z., Tan,S.H., O'Connor,M.J. and Bernard,H.U. (2000) Nuclear matrix attachment regions of human papillomavirus type 16 repress or activate the E6 promoter, depending on the physical state of the viral DNA. *J. Virol.*, **74**, 2489–2501.
14. Tan,S.H., Bartsch,D., Schwarz,E. and Bernard,H.U. (1998) Nuclear matrix attachment regions of human papillomavirus type 16 point toward conservation of these genomic elements in all genital papillomaviruses. *J. Virol.*, **72**, 3610–3622.
15. Schaack,J., Ho,W.Y., Freimuth,P. and Shenk,T. (1990) Adenovirus terminal protein mediates both nuclear matrix association and efficient transcription of adenovirus DNA. *Genes Dev.*, **4**, 1197–1208.
16. Krithivas,A., Fujimuro,M., Weidner,M., Young,D.B. and Hayward,S.D. (2002) Protein interactions targeting the latency-associated nuclear antigen of Kaposi's sarcoma-associated herpesvirus to cell chromosomes. *J. Virol.*, **76**, 11596–11604.
17. D'Ugo,E., Bruni,R., Argentini,C., Giuseppetti,R. and Rapicetta,M. (1998) Identification of scaffold/matrix attachment region in recurrent site of woodchuck hepatitis virus integration. *DNA Cell Biol.*, **17**, 519–527.
18. Shera,K.A., Shera,C.A. and McDougall,J.K. (2001) Small tumor virus genomes are integrated near nuclear matrix attachment regions in transformed cells. *J. Virol.*, **75**, 12339–12346.
19. Jenke,B.H., Fetzer,C.P., Stehle,I.M., Jonsson,F., Fackelmayer,F.O., Conradt,H., Bode,J. and Lipps,H.J. (2002) An episomally replicating vector binds to the nuclear matrix protein SAF-A *in vivo*. *EMBO Rep.*, **3**, 349–354.
20. Piechaczek,C., Fetzer,C., Baiker,A., Bode,J. and Lipps,H.J. (1999) A vector based on the SV40 origin of replication and chromosomal S/MARs replicates episomally in CHO cells. *Nucleic Acids Res.*, **27**, 426–428.
21. Baiker,A., Maercker,C., Piechaczek,C., Schmidt,S.B., Bode,J., Benham,C. and Lipps,H.J. (2000) Mitotic stability of an episomal vector containing a human scaffold/matrix-attached region is provided by association with nuclear matrix. *Nat. Cell Biol.*, **2**, 182–184.
22. Dean,D.A. (1997) Import of plasmid DNA into the nucleus is sequence specific. *Exp. Cell Res.*, **230**, 293–302.
23. Jiao,R., Yu,W., Ding,M. and Zhai,Z. (1992) Localization of adenovirus DNA by in situ hybridization electron microscopy. *Microsc. Res. Tech.*, **21**, 23–31.
24. Nielsen,P.E., Egholm,M., Berg,R.H. and Buchardt,O. (1991) Sequence-selective recognition of DNA by strand displacement with a thymine-substituted polyamide. *Science*, **254**, 1497–1500.
25. Hyrup,B. and Nielsen,P.E. (1996) Peptide nucleic acids (PNA): synthesis, properties and potential applications. *Bioorg. Med. Chem.*, **4**, 5–23.
26. Egholm,M., Buchardt,O., Christensen,L., Behrens,C., Freier,S.M., Driver,D.A., Berg,R.H., Kim,S.K., Norden,B. and Nielsen,P.E. (1993) PNA hybridizes to complementary oligonucleotides obeying the Watson–Crick hydrogen-bonding rules. *Nature*, **365**, 566–568.
27. Demidov,V.V., Potaman,V.N., Frank-Kamenetskii,M.D., Egholm,M., Buchard,O., Sonnichsen,S.H. and Nielsen,P.E. (1994) Stability of peptide nucleic acids in human serum and cellular extracts. *Biochem. Pharmacol.*, **48**, 1310–1313.
28. Nielsen,P.E., Egholm,M. and Buchardt,O. (1994) Evidence for (PNA)2/DNA triplex structure upon binding of PNA to dsDNA by strand displacement. *J Mol Recognit.*, **7**, 165–170.
29. Nielsen,P.E. (2001) Targeting double stranded DNA with peptide nucleic acid (PNA). *Curr. Med. Chem.*, **8**, 545–550.
30. Zelphati,O., Liang,X., Hobart,P. and Felgner,P.L. (1999) Gene chemistry: functionally and conformationally intact fluorescent plasmid DNA. *Hum. Gene Ther.*, **10**, 15–24.
31. Nielsen,P.E. (2000) Peptide nucleic acids: on the road to new gene therapeutic drugs. *Pharmacol. Toxicol.*, **86**, 3–7.
32. Romig,H., Ruff,J., Fackelmayer,F.O., Patil,M.S. and Richter,A. (1994) Characterisation of two intronic nuclear-matrix-attachment regions in the human DNA topoisomerase I gene. *Eur. J. Biochem.*, **221**, 411–419.
33. Fackelmayer,F.O. and Richter,A. (1994) hnRNP-U/SAF-A is encoded by two differentially polyadenylated mRNAs in human cells. *Biochim. Biophys. Acta*, **1217**, 232–234.
34. Christensen,L., Fitzpatrick,R., Gildea,B., Petersen,K.H., Hansen,H.F., Koch,T., Egholm,M., Buchardt,O., Nielsen,P.E., Coull,J. *et al.* (1995) Solid-phase synthesis of peptide nucleic acids. *J. Pept. Sci.*, **1**, 175–183.

35. Renz,A. and Fackelmayer,F.O. (1996) Purification and molecular cloning of the scaffold attachment factor B (SAF-B), a novel human nuclear protein that specifically binds to S/MAR-DNA. *Nucleic Acids Res.*, **24**, 843–849.
36. Fackelmayer,F.O., Dahm,K., Renz,A., Ramsperger,U. and Richter,A. (1994) Nucleic-acid-binding properties of hnRNP-U/SAF-A, a nuclear-matrix protein which binds DNA and RNA *in vivo* and *in vitro*. *Eur. J. Biochem.*, **221**, 749–757.
37. Neri,L.M., Zweyer,M., Falcieri,E., Bortul,R. and Martelli,A.M. (1997) Changes in the subnuclear distribution of two RNA metabolism-related proteins can be detected in nuclear scaffold or matrix prepared by different techniques. *Histochem. Cell Biol.*, **108**, 525–536.
38. Wang,G., Xu,X., Pace,B., Dean,D.A., Glazer,P.M., Chan,P., Goodman,S.R. and Shokolenko,I. (1999) Peptide nucleic acid (PNA) binding-mediated induction of human gamma-globin gene expression. *Nucleic Acids Res.*, **27**, 2806–2813.
39. Egholm,M., Christensen,L., Dueholm,K.L., Buchardt,O., Coull,J. and Nielsen,P.E. (1995) Efficient pH-independent sequence-specific DNA binding by pseudoisocytosine-containing bis-PNA. *Nucleic Acids Res.*, **23**, 217–222.
40. Bentin,T., Larsen,H.J. and Nielsen,P.E. (2003) Combined triplex/duplex invasion of double-stranded DNA by 'tail-clamp' peptide nucleic acid. *Biochemistry*, **42**, 13987–13995.
41. Marashi,F., Stein,G.S., Stein,J.L. and Schubert,C. (1985) Use of ultrafiltration microconcentrators in the concentration and desalting of DNA. *Biotechniques*, **3**, 238–240.
42. Gorisch,S.M., Richter,K., Scheuermann,M.O., Herrmann,H. and Lichter,P. (2003) Diffusion-limited compartmentalization of mammalian cell nuclei assessed by microinjected macromolecules. *Exp. Cell Res.*, **289**, 282–294.
43. Braun,K., Peschke,P., Pipkorn,R., Lampel,S., Wachsmuth,M., Waldeck,W., Friedrich,E. and Debus,J. (2002) A biological transporter for the delivery of peptide nucleic acids (PNAs) to the nuclear compartment of living cells. *J. Mol. Biol.*, **318**, 237–243.
44. Matera,A.G. (1999) Nuclear bodies: multifaceted subdomains of the interchromatin space. *Trends Cell Biol.*, **9**, 302–309.
45. Kipp,M., Göhring,F., Ostendorp,T., van Drunen,C.M., van Driel,R., Przybylski,M. and Fackelmayer,F.O. (2000) SAF-Box, a conserved protein domain that specifically recognizes scaffold attachment region DNA. *Mol. Cell. Biol.*, **20**, 7480–7489.
46. Göhring,F., Schwab,B.L., Nicotera,P., Leist,M. and Fackelmayer,F.O. (1997) The novel SAR-binding domain of scaffold attachment factor A (SAF-A) is a target in apoptotic nuclear breakdown. *EMBO J.*, **16**, 7361–7371.
47. Romig,H., Fackelmayer,F.O., Renz,A., Ramsperger,U. and Richter,A. (1992) Characterization of SAF-A, a novel nuclear DNA binding protein from HeLa cells with high affinity for nuclear matrix/scaffold attachment DNA elements. *EMBO J.*, **11**, 3431–3440.
48. Martelli,A.M., Cocco,L., Riederer,B.M. and Neri,L.M. (1996) The nuclear matrix: A critical appraisal. *Histol. Histopathol.*, **11**, 1035–1048.
49. Daigle,N., Beaudouin,J., Hartnell,L., Imreh,G., Hallberg,E., Lippincott-Schwartz,J. and Ellenberg,J. (2001) Nuclear pore complexes form immobile networks and have a very low turnover in live mammalian cells. *J. Cell Biol.*, **154**, 71–84.
50. Misteli,T. (2001) Protein dynamics: implications for nuclear architecture and gene expression. *Science*, **291**, 843–847.
51. Misteli,T. and Spector,D.L. (1997) Applications of the green fluorescent protein in cell biology and biotechnology. *Nat. Biotechnol.*, **15**, 961–964.
52. Kanda,T., Sullivan,K.F. and Wahl,G.M. (1998) Histone-GFP fusion protein enables sensitive analysis of chromosome dynamics in living mammalian cells. *Curr. Biol.*, **8**, 377–385.
53. Robinett,C.C., Straight,A., Li,G., Willhelm,C., Sudlow,G., Murray,A. and Belmont,A.S. (1996) *In vivo* localization of DNA sequences and visualization of large-scale chromatin organization using *lac* operator/repressor recognition, *J. Cell Biol.*, **135**, 1685–1700.
54. Gasser,S.M. (2002) Visualizing chromatin dynamics in interphase nuclei. *Science*, **296**, 1412–1416.
55. Zink,D., Cremer,T., Saffrich,R., Fischer,R., Trendelenburg,M.F., Ansorge,W. and Stelzer,E.H. (1998) Structure and dynamics of human interphase chromosome territories *in vivo*. *Hum. Genet.*, **102**, 241–251.
56. Cremer,T., Kreth,G., Koester,H., Fink,R.H., Heintzmann,R., Cremer,M., Solovei,I., Zink,D. and Cremer,C. (2000) Chromosome territories, interchromatin domain compartment and nuclear matrix: an integrated view of the functional nuclear architecture. *Crit. Rev. Eukaryot. Gene Expr.*, **10**, 179–212.
57. Berezney,R., Mortillaro,M.J., Ma,H., Wei,X. and Samarabandu,J. (1995) The nuclear matrix: a structural milieu for genomic function. *Int. Rev. Cytol.*, **162A**, 1–65.
58. DePamphilis,M.L. (2000) Review: nuclear structure and DNA replication. *J. Struct. Biol.*, **129**, 186–197.
59. Stenoien,D.L., Patel,K., Mancini,M.G., Dutertre,M., Smith,C.L., O'Malley,B.W. and Mancini,M.A. (2001) FRAP reveals that mobility of oestrogen receptor-alpha is ligand- and proteasome-dependent. *Nat. Cell Biol.*, **3**, 15–23.
60. Calapez,A., Pereira,H.M., Calado,A., Braga,J., Rino,J., Carvalho,C., Tavanez,J.P., Wahle,E., Rosa,A.C. and Carmo-Fonseca,M. (2002) The intranuclear mobility of messenger RNA binding proteins is ATP dependent and temperature sensitive. *J. Cell Biol.*, **159**, 795–805.
61. Lukacs,G.L., Haggie,P., Seksek,O., Lechardeur,D., Freedman,N. and Verkman,A.S. (2000) Size-dependent DNA mobility in cytoplasm and nucleus. *J. Biol. Chem.*, **275**, 1625–1629.
62. Luderus,M.E., de Graaf,A., Mattia,E., den Blaauwen,J.L., Grande,M.A., de Jong,L. and van Driel,R. (1992) Binding of matrix attachment regions to lamin B1. *Cell*, **70**, 949–959.
63. Hakes,D.J. and Berezney,R. (1991) DNA binding properties of the nuclear matrix and individual nuclear matrix proteins. Evidence for salt-resistant DNA binding sites. *J. Biol. Chem.*, **266**, 11131–11140.
64. Kay,V. and Bode,J. (1994) Binding specificity of a nuclear scaffold: supercoiled, single-stranded and scaffold-attached-region DNA. *Biochemistry*, **33**, 367–374.
65. vanWijnen,A.J., Bidwell,J.P., Fey,E.G., Penman,S., Lian,J.B., Stein,J.L. and Stein,G.S. (1993) Nuclear matrix association of multiple sequence-specific DNA binding activities related to SP-1, ATF, CCAAT, C/EBP, OCT-1 and AP-1. *Biochemistry*, **32**, 8397–8402.
66. Christensen,M.O., Larsen,M.K., Barthelmes,H.U., Hock,R., Andersen,C.L., Kjeldsen,E., Knudsen,B.R., Westergaard,O., Boege,F. and Mielke,C. (2002) Dynamics of human DNA topoisomerases IIalpha and IIbeta in living cells. *J. Cell Biol.*, **157**, 31–44.
67. Jackson,D.A. and Cook,P.R. (1993) Transcriptionally active minichromosomes are attached transiently in nuclei through transcription units. *J. Cell Sci.*, **105**, 1143–1150.
68. Weipoltshammer,K., Schofer,C., Wachtler,F. and Hozak,P. (1996) The transcription unit of ribosomal genes is attached to the nuclear skeleton. *Exp. Cell Res.*, **227**, 374–379.
69. Iborra,F., Pombo,A., Jackson,D. and Cook,P. (1996) Active RNA polymerases are localized within discrete transcription 'factories' in human nuclei. *J Cell Sci*, **109**, 1427–1436.
70. Nayler,O., Stratling,W., Bourquin,J.P., Stagljar,I., Lindemann,L., Jasper,H., Hartmann,A.M., Fackelmayer,F.O., Ullrich,A. and Stamm,S. (1998) SAF-B protein couples transcription and pre-mRNA splicing to SAR/MAR elements. *Nucleic Acids Res.*, **26**, 3542–3549.